

Pair interaction potentials with explicit polarization for molecular dynamics simulations of La^{3+} in bulk water

Magali Duvail, Marc Souaille, Riccardo Spezia, and Thierry Cartailier

Laboratoire Analyse et Modélisation pour la Biologie et l'Environnement, CNRS UMR 8587, Université d'Evry Val d'Essonne, Boulevard F. Mitterrand, 91025 Evry Cedex, France

Pierre Vitorge^{a)}

CEA Saclay, DEN/DPC/SECR/LSRM, 91991 Gif Sur Yvette, France

(Received 3 April 2007; accepted 31 May 2007; published online 19 July 2007)

Pair interaction potentials (IPs) were defined to describe the $\text{La}^{3+}-\text{OH}_2$ interaction for simulating the La^{3+} hydration in aqueous solution. $\text{La}^{3+}-\text{OH}_2$ IPs are taken from the literature or parametrized essentially to reproduce *ab initio* calculations at the second-order Møller-Plesset level of theory on $\text{La}(\text{H}_2\text{O})_8^{3+}$. The IPs are compared and used with molecular dynamics (MD) including explicit polarization, periodic boundary conditions of $\text{La}(\text{H}_2\text{O})_{216}^{3+}$ boxes, and TIP3P water model modified to include explicit polarization. As expected, explicit polarization is crucial for obtaining both correct La–O distances ($r_{\text{La-O}}$) and La^{3+} coordination number (CN). Including polarization also modifies hydration structure up to the second hydration shell and decreases the number of water exchanges between the La^{3+} first and second hydration shells. $r_{\text{La-O}}^{(1)}=2.52$ Å and $\text{CN}^{(1)}=9.02$ are obtained here for our best potential. These values are in good agreement with experimental data. The tested La–O IPs appear to essentially account for the La–O short distance repulsion. As a consequence, we propose that most of the multibody effects are correctly described by the explicit polarization contributions even in the first La^{3+} hydration shell. The MD simulation results are slightly improved by adding a—typically negative $1/r^6$ —slightly attractive contribution to the—typically exponential—repulsive term of the La–O IP. Mean residence times are obtained from MD simulations for a water molecule in the first (1082 ps) and second (7.6 ps) hydration shells of La^{3+} . The corresponding water exchange is a concerted mechanism: a water molecule leaving $\text{La}(\text{H}_2\text{O})_9^{3+}$ in the opposite direction to the incoming water molecule. $\text{La}(\text{H}_2\text{O})_9^{3+}$ has a slightly distorted “6 + 3” tricapped trigonal prism D_{3h} structure, and the weakest bonding is in the medium triangle, where water exchanges take place. © 2007 American Institute of Physics.
[DOI: 10.1063/1.2751503]

I. INTRODUCTION

Lanthanide aqueous trications (Ln^{3+}) have similar chemical behaviors. Their hydration structure has been studied by means of classical,^{1–13} quantum mechanical/molecular mechanical (QM/MM),¹⁴ Car-Parinello molecular dynamics (CPMD),¹⁵ and Monte Carlo (MC) simulations.^{2,16} Classical molecular dynamics (CLMD) simulations can give realistic pictures of hydrated ion structures and dynamics with a relatively low computational cost for simulations up to nanoseconds, a long enough time scale to study exchanges of water molecules in the Ln^{3+} first hydration shell. The corresponding mean residence times (MRTs) are out of reach of QM/MM (Ref. 14) and CPMD (Ref. 15) simulations. CLMD is now able to settle such time scales using analytical interaction potentials (IPs) that need to be parametrized.

Such IPs can be built to reproduce *ab initio* calculations on systems containing only two molecules, namely, actual pair IPs as suggested in two recently published works,^{10,11}

where different sizes of La^{3+} water clusters were investigated. In Ref. 17, relatively small clusters (up to nine water molecules with one central Ln^{3+} cation) were studied. Unfortunately, this study did not reproduce the experimental coordination number (CN) of the cation in liquid water, while bigger systems were studied a little later by the same group¹⁰ using another force field which provided better results. To our best knowledge, IPs have not been used with explicit polarization and periodic boundary conditions, while such an approach has been limited to big clusters up to 128 water molecules with one central Ln^{3+} cation.^{10–12} The advantage of such physical approaches is to provide transferable atomic parameters, since these parameters correspond to atomic intrinsic properties. Nevertheless, in both force fields a short range repulsive term was empirically added.^{10–12} When parametrizing their potential for earlier MC simulations, Galera *et al.*² have pointed out that the $1/r^{12}$ term in the Lennard-Jones potentials leads to a repulsion that is too strong, whereas the exponential term in the second potential is too weak, albeit a globally good description of structural parameters for lanthanide aqua ions was obtained.

In another approach, the pair IPs have been parametrized to exactly reproduce *ab initio* calculations. For this, many

^{a)}Also at Laboratoire Analyse et Modélisation pour la Biologie et l'Environnement, CNRS UMR 8587, Université d'Evry Val d'Essonne, Boulevard F. Mitterrand, 91025 Evry Cedex, France. Electronic mail: pierre.vitorge@cea.fr

parameters were fitted, but this did not completely reproduce experimental results of $\text{Ln}^{3+}/\text{H}_2\text{O}$ systems.⁸ Pair IPs have also been successfully parametrized to exactly reproduce the available macroscopic experimental results.^{9,13}

Actually, the first pleasing results for Ln^{3+} hydration MD simulations were obtained more than ten years ago by using a pragmatic mixed approach, where the model potentials were tentatively fitted on *ab initio* partial potential energy surfaces but further rescaled after short time trial simulations by comparison with macroscopic properties.^{3-5,7} Polarization effects were taken into account semiempirically to be within the reach of MD simulations carried out on workstations during 1994. The polarization procedure was scaled on *ab initio* calculations at the HF level of theory on $\text{Ln}(\text{H}_2\text{O})_8^{3+}$ clusters and one second-order Møller-Plesset (MP2) calculation.⁵ As a result of such a rescaling, the fitting procedure provides phenomenological or bulk rather than actual ion pair and purely atomic physical parameters. However, such an approach is consistent with the use of well established water models, such as TIP3P, among the most simple ones. For consistency with the rescaling, the *ab initio* calculations were performed on $\text{Ln}(\text{H}_2\text{O})_8^{3+}$ big enough clusters to parametrize the $\text{Ln}^{3+}-\text{OH}_2$ IP and not only on $\text{Ln}(\text{H}_2\text{O})^{3+}$.

Thus, as suggested by literature investigation, MD simulations should explicitly include all polarization effects. They should also be based on $\text{Ln}^{3+}-\text{OH}_2$ IPs parametrized (or checked) in order to reproduce high level quantum calculations of big enough clusters, typically of the $\text{Ln}(\text{H}_2\text{O})_8^{3+}$ size, so that bulk effects can be correctly described. This is because there is no well established theoretical reason for choosing the mathematical form of the repulsion term—typically exponential or $1/r^n$. Supplementary physical terms are usually added as typically $1/r^6$ attractive ones for dispersion; unfortunately, they might as well compensate for systematic errors of the short range repulsion term (because the correct mathematical form of the repulsion term is not undebatable for the interaction of highly charged cations with water). However, the ingredients for realistic MD simulations have not really been put together for a single study on a $\text{Ln}^{3+}/\text{H}_2\text{O}$ system, i.e., periodic boundary conditions, explicit polarization, and $\text{Ln}^{3+}-\text{OH}_2$ interaction potentials that reproduce high level quantum chemistry calculations. For this reason it is now tempting to gather the above simulation methodologies in a single approach and to compare the simulation results to well established experimental data. This approach is presented here. For this, we used our own MD code where all these features are implemented.¹⁸ An objective of this paper was to test the MD code with a highly charged Ln^{3+} cation and with a water maximum residence time that can be naturally observed during MD simulations. Thus, different IPs have also been compared.

To simplify the quantum chemistry calculations used to parametrize IPs, we have chosen La^{3+} , the lanthanide with the simplest electronic configuration, i.e., closed shell with no *f* electron. It is a chemical analog of the other lanthanides (III). Lanthanides are essentially stable at the +3 oxidation state and have similar behaviors in aqueous solutions. This analogy is usually attributed to the hardness of the Ln^{3+} ions: their coordinations mainly depend on the steric and electro-

static nature of the ligand interactions.¹⁹ For the same reason, the 4*f*-block lanthanide elements are also chemical analogs of the 5*f*-block actinide elements, when at the same oxidation state.²⁰⁻²⁵ Actually, in the nuclear fuel cycle industry, it is a challenge to separate the Am and Cm actinide activation products from (light) lanthanide fission products in an attempt to eliminate long live radionuclides from radioactive wastes. Furthermore, analogies between hard cations at the same oxidation states are currently used as rough estimates for the thermodynamic stabilities of their aqueous hydroxides and complexes with (inorganic) ligands of the underground waters about possible waste repositories.²⁵⁻²⁸ The stoichiometries and stabilities of aqueous chemical species are needed to model the solubilities and migrations of radionuclides. The knowledge of hydration is thus the first step needed for the theoretical studies of such chemical reactions.

The $\text{La}-\text{OH}_2$ distance ($r_{\text{La}-\text{O}}$) is well known in water and has been measured by extended x-ray absorption fine structure (EXAFS) spectroscopy in concentrated Cl^- and ClO_4^- aqueous solutions.^{22,29-31} Results are in the 2.54–2.56 Å range. This confirms earlier measurements (2.48–2.58 Å) by x-ray diffraction³²⁻³⁴ (XRD) but with slightly better accuracy. In the treatment of these XRD or EXAFS experimental data, values were fixed or fitted in the range of 8–12 for the CN of La^{3+} . The $r_{\text{La}-\text{O}}$ determinations do not seem to be especially correlated to such CN values, neither to the aqueous concentration of the Cl^- nor ClO_4^- counteranion (less than 2 mol kg^{-1}). This illustrates that the exact stoichiometry and structure of $\text{La}^{3+}(\text{aq})$ cannot be deduced from such experimental results alone; only $r_{\text{La}-\text{O}}$ is well established being in the range of 2.54–2.56 Å.

As outlined above, in published CLMD studies, the IPs have also been built on more qualitative—actually even quite speculative—experimental information and corresponding interpretation. This experimental information has recently been reviewed by Helm and Merbach (see Ref. 35 and reference therein). From such reviews it is concluded that the stoichiometry of the first La^{3+} hydration shell is $\text{La}(\text{H}_2\text{O})_9^{3+}$ (hence CN=9) and that the MRT is not known for a water molecule in this first La^{3+} hydration shell. MRTs have been extracted from ¹⁷O NMR measurements only for heavier lanthanides,^{3,19,35-40} whose stoichiometry is different [$\text{Ln}(\text{H}_2\text{O})_8^{3+}$]. For this reason, such measurements cannot be extrapolated to $\text{La}(\text{H}_2\text{O})_9^{3+}$. However, similar water residence times were found for $\text{Ln}^{3+}(\text{aq})$ and $\text{LnSO}_4^+(\text{aq})$ as extracted from NMR (Refs. 37, 41, and 42) and ultrasonic absorption⁴³ (UA) measurements, respectively. For this reason, it has been suggested³⁶ that the residence time in $\text{LaSO}_4^+(\text{aq})$ is a good approximation of that in $\text{La}^{3+}(\text{aq})$, namely, 4.8 ns as reinterpreted from an original 1.9 ns value. Nevertheless, this hypothesis needs confirmation, since this analogy [between $\text{Ln}^{3+}(\text{aq})$ and $\text{LnSO}_4^+(\text{aq})$] was only observed when $\text{Ln}^{3+}(\text{aq})=\text{Ln}(\text{H}_2\text{O})_8^{3+}(\text{aq})$, while experimental data are missing for $\text{Ln}^{3+}(\text{aq})=\text{Ln}(\text{H}_2\text{O})_9^{3+}(\text{aq})$. Furthermore, shorter residence times are obtained from published MD as compared to the experimental values, as outlined above by Kowall *et al.*⁵ when discussing their pioneering results. The same effect is observed for the later MD published data,^{8,10} when compared with NMR (Refs. 36, 37, 42, and 44) or UA (Ref. 43) ex-

TABLE I. Parameters used for the CLMD simulations. Energies are in kJ mol⁻¹, distances in Å, and atomic polarizabilities in Å³.

Ion/water	IP	ϵ_{O-O}	σ_{O-O}	A_{ij}	B_{ij}	$C_{6,ij}$	$C_{8,ij}$	$C_{10,ij}$	q_i	α
La ³⁺	Exp			$5.111 \times 10^{+5}$	3.50				+3.000	1.41
La ³⁺	Exp _{up}			$5.805 \times 10^{+5}$	3.86				+3.000	1.41
La ³⁺	Buck6			$1.004 \times 10^{+6}$	3.48	$3.766 \times 10^{+4}$			+3.000	1.41
La ³⁺	Buck6 _{up}			$1.046 \times 10^{+6}$	3.50	$3.975 \times 10^{+4}$			+3.000	1.41
La ³⁺	TF			$-6.576 \times 10^{+3}$	1.27	$-9.206 \times 10^{+4}$	$1.234 \times 10^{+5}$	$-1.745 \times 10^{+4}$	+3.000	1.41
La ³⁺	TF _{up}			$6.474 \times 10^{+5}$	3.06	$1.322 \times 10^{+5}$	$-2.821 \times 10^{+5}$	$2.210 \times 10^{+5}$	+3.000	1.41
La ³⁺	Kit			2.309×10^6	4.119	3.843×10^3	9.205×10^3	2.976×10^4	+3.000	1.41
O _w	TIP3P/P	0.510	3.165						-0.658	0.85
O _w	TIP3P	0.649	3.165						-0.834	0.85
O _w	Kit			8.576×10^5	3.984	9.821×10^2	2.515×10^3	8.690×10^3	-0.834	0.85
H _w	TIP3P/P								+0.329	0.41
H _w	TIP3P								+0.417	0.41

perimental data. The origin of this problem is not clear. For this reason, we will not specially use MRTs to evaluate the quality of simulations. However, we can provide a dynamical picture based on an IP yielding reliable structural data.

The outline of the remainder of the text is as follows. We first describe the model potential forms used (Sec. II A), then the *ab initio* calculation procedure (Sec. II B), and we present the MD simulation details (Sec. II C). Results and discussion are presented in Sec. III, where we first discuss the different potentials used (Sec. III A) and then the influence of the polarization (Sec. III B). Finally, the hydration structure of La³⁺ at room temperature (Sec. III C) and its dynamics (Sec. III D) are described.

II. METHODS

A. Model potentials

The total energy of our system is modeled as a sum of potential energy terms,

$$V_{\text{tot}} = V_{\text{elec}} + V_{\text{O-O}}^{\text{LJ}} + V_{\text{La-O}}, \quad (1)$$

where V_{elec} is the electrostatic energy term composed of the solvent-solvent and solvent-solute interactions,

$$V_{\text{elec}} = \frac{1}{2} \sum_{i,j,i \neq j} \left[\frac{q_i q_j}{r_{ij}} + \frac{1}{r_{ij}^3} (-q_i \mathbf{p}_j + q_j \mathbf{p}_i) \cdot \mathbf{r}_{ij} + \mathbf{p}_i \cdot \bar{\bar{\mathbf{T}}}_{ij} \cdot \mathbf{p}_j \right] + \frac{1}{2} \sum_i \mathbf{p}_i \cdot (\bar{\bar{\alpha}}_i)^{-1} \cdot \mathbf{p}_i, \quad (2)$$

where, following Thole's induced dipole model,⁴⁵ each atomic site i carries one permanent charge q_i and one induced dipole \mathbf{p}_i associated with an isotropic atomic polarizability tensor $\bar{\bar{\alpha}}_i$, $\mathbf{r}_{ij} = \mathbf{r}_i - \mathbf{r}_j$,

$$\bar{\bar{\mathbf{T}}}_{ij} = \frac{1}{r_{ij}^3} \left(\bar{\bar{\mathbf{1}}} - 3 \frac{\mathbf{r}_{ij} \mathbf{r}_{ij}}{r_{ij}^2} \right), \quad (3)$$

and $1/2 \sum_i \mathbf{p}_i \cdot (\bar{\bar{\alpha}}_i)^{-1} \cdot \mathbf{p}_i$ is the polarization energy. As previously mentioned, we used Thole's model where the polarization catastrophe is avoided using a screening function for the dipole-dipole interactions at short distances. Here we adopted the exponential form among the originally proposed

screening functions because of its continuous character (also shared by its derivatives), so that the electrostatic potential is now

$$V_{\text{elec}} = \frac{1}{2} \sum_{i,j,i \neq j} (q_i + \mathbf{p}_i \cdot \nabla_i) (q_j - \mathbf{p}_j \cdot \nabla_j) \phi^s(r_{ij}) + \frac{1}{2} \sum_i \mathbf{p}_i \cdot (\bar{\bar{\alpha}}_i)^{-1} \cdot \mathbf{p}_i, \quad (4)$$

where $\phi^s(r_{ij})$ is the screened electrostatic potential,

$$\phi^s(r_{ij}) = \frac{1}{r_{ij}} \left[1 - \left(1 + \frac{au}{2} \right) e^{-au} \right], \quad (5)$$

with $u = r_{ij}/(\alpha_i \alpha_j)^{1/6}$ and $a = 2.1304 \text{ \AA}^{-1}$ as determined in the original work.⁴⁵ Isotropic polarizabilities are assigned at each atomic site. Here we used atomic polarizabilities determined by van Duijnen and Swart⁴⁶ for O (0.85 \AA^3) and H (0.41 \AA^3), and for La³⁺ the tabulated value⁴⁷ of 1.41 \AA^3 (see Table I). The induced dipoles are obtained through the resolution of the self-consistent equations

$$\mathbf{p}_i = \bar{\bar{\alpha}}_i \cdot \left(\mathbf{E}_i + \sum_{i \neq j} \bar{\bar{\mathbf{T}}}_{ij} \cdot \mathbf{p}_j \right). \quad (6)$$

The resolution of this self-consistent problem becomes rapidly extremely time consuming as the system grows. In order to reduce the computing time, we have used an alternative way of resolving such a problem for each time step of the dynamics. In particular, we have used a Car-Parrinello type of dynamics⁴⁸ of additional degrees of freedom associated with induced dipoles.⁴⁹ Thus, the Hamiltonian of the system is now

$$\mathcal{H} = V + \frac{1}{2} \sum_i m_i \mathbf{v}_i^2 + \frac{1}{2} \sum_i m_{\mathbf{p}_i} \mathbf{v}_{\mathbf{p}_i}^2, \quad (7)$$

where V is the total potential, \mathbf{v}_i is the velocity of the atom i , $\mathbf{v}_{\mathbf{p}_i}$ is the velocity of the induced dipole \mathbf{p}_i treated as an additional degree of freedom in the dynamics, and $m_{\mathbf{p}_i}$ is its associated fictitious mass (identical for each atom). Dynamics of the induced dipole degrees of freedom is fictitious, such that it only serves the purpose of keeping the induced dipoles close to their values at the minimum energy (that would be obtained through the exact resolution of self-

consistent equations). Thus, induced dipole dynamics adiabatically follows the nuclei dynamics if a proper choice of the fictitious mass is done. A decoupling or at least a very weak coupling, between nuclei degrees of freedom and fictitious dipole degrees of freedom, is needed to maintain adiabaticity. Fictitious masses are connected to characteristic frequencies of the induced dipoles,

$$\omega_{\mathbf{p}_i} = \frac{2\pi}{\tau} = \frac{1}{\sqrt{m_{\mathbf{p}_i} \alpha_i}}, \quad (8)$$

that are set here to be $\tau=0.005$ ps for each atomic site. Further details are given in Ref. 18.

$V_{\text{O-O}}^{\text{LJ}}$ in Eq. (1) is the 12-6 Lennard-Jones (LJ) potential⁵⁰ describing the O-O interaction of TIP3P water molecules.⁵¹

$$V_{ij}^{\text{LJ}} = \sum_{i,j} 4\epsilon_{ij} \left[\left(\frac{\sigma_{ij}}{r_{ij}} \right)^{12} - \left(\frac{\sigma_{ij}}{r_{ij}} \right)^6 \right]. \quad (9)$$

The partial atomic charges in O and H of the original TIP3P water model had been optimized to reproduce water properties based on models without polarization,⁵¹ containing only an electrostatic term and a 12-6 LJ term. Introducing a polarization term in the model will overestimate the water dipole moment. Consequently, a scaling factor is introduced on the partial atomic charges to reproduce the experimental dipole moment of water as done by Caldwell *et al.*^{52,53} and Armunanto *et al.*⁵⁴ By recalculating this scaling factor, we obtained atomic partial charges on O and H of $-0.658e$ and $+0.329e$, respectively (Table I). This model is here called the TIP3P/P model. Namely, two water models were used: (i) the TIP3P/P model including the V_{pol} term and (ii) the original TIP3P model when polarization term is not added on the electrostatic interaction, i.e., in the latter case the electrostatic term is only composed of a Coulomb term.

$V_{\text{La-O}}$ account for the *nonelectrostatic* La-O interactions. Several potential forms were tested to describe these interactions. First, the purely repulsive exponential (Exp) potential,

$$V_{ij}^{\text{Exp}} = A_{ij}^{\text{Exp}} \exp(-B_{ij}^{\text{Exp}} r_{ij}), \quad (10)$$

where A_{ij}^{Exp} and B_{ij}^{Exp} are fitted parameters. Then, the Buckingham exponential-6 (Buck6) potential,⁵⁵

$$V_{ij}^{\text{Buck6}} = A_{ij}^{\text{Buck6}} \exp(-B_{ij}^{\text{Buck6}} r_{ij}) - \frac{C_{6,ij}^{\text{Buck6}}}{r_{ij}^6}, \quad (11)$$

where the fitted parameters are A_{ij}^{Buck6} , B_{ij}^{Buck6} , and $C_{6,ij}^{\text{Buck6}}$. Finally, the Tosi-Fumi (TF) potential,^{56,57}

$$V_{ij}^{\text{TF}}(r_{ij}) = A_{ij}^{\text{TF}} \exp(-B_{ij}^{\text{TF}} r_{ij}) - \frac{C_{6,ij}^{\text{TF}}}{r_{ij}^6} - \frac{C_{8,ij}^{\text{TF}}}{r_{ij}^8} - \frac{C_{10,ij}^{\text{TF}}}{r_{ij}^{10}}, \quad (12)$$

where the fitted parameters are A_{ij}^{TF} , B_{ij}^{TF} , $C_{6,ij}^{\text{TF}}$, $C_{8,ij}^{\text{TF}}$, and $C_{10,ij}^{\text{TF}}$. For these three La-O IPs, the parameters were fitted on MP2 *ab initio* calculations of $\text{La}(\text{H}_2\text{O})^{3+}$ and/or $\text{La}(\text{H}_2\text{O})_8^{3+}$ and eventually refined on MD simulations (see Secs. II B and III A for details). The resulting values are shown in Table I. We also tested the Kitaygorodsky (Kit) potential⁵⁸ describing both the La-water and the water-water *nonelectrostatic* interactions,

$$V_{\text{int}}^{\text{Kit}} = \sum_i \sum_j k_i k_j \left(G_{ij} C \exp(-\gamma z) - \left(\frac{C_6}{z^6} + \frac{C_8}{z^8} + \frac{C_{10}}{z^{10}} \right) + G_{ij} C^{de} \exp(-\gamma^{de} z) \right), \quad (13)$$

where

$$z = \frac{r_{ij}}{r_{ij}^0} \quad (14)$$

and

$$r_{ij}^0 = \sqrt{(2R_i^w)(2R_j^w)}, \quad (15)$$

where R_i^w and R_j^w are the van der Waals radii. Here, the numerical values of the parameters are assumed to reflect actual atomic properties, for this reason they should be fitted on various molecules. Here we have used the original Derepas parameters.^{17,59} In the Kit expression

$$G_{ij} = \left(1 - \frac{q_i}{n_i^{\text{val}}} \right) \left(1 - \frac{q_j}{n_j^{\text{val}}} \right), \quad (16)$$

where q_i is the partial atomic charge of atom i and n_i^{val} is the number of valence electrons of atom i . Note that parameters C_6 , C_8 , C_{10} , C , C^{de} , γ , and γ^{de} are independent of the atomic species i and j (Table I). For comparing only the Kit La-O IP with our best potentials, we performed simulations with (i) the Kit potential for all interactions and (ii) the Kit only for the La^{3+} -O interaction and the TIP3P/P model for the O-O water interactions. This modified Kit potential is here called Kit-TIP3P/P potential.

We have also tested a 12-6 LJ potential [Eq. (9)] for the La-O IP. This gave poor results, and we finally did not use this kind of potential for the La-O interaction.

B. *Ab initio* calculations

The La-O interaction energies fitted by using the analytic functions described in Sec. II A were obtained from calculated *ab initio* potential energy surfaces (PES) scan. Symmetric model $\text{La}(\text{H}_2\text{O})_8^{3+}$ clusters were built (Fig. 1), where the La-O distances were equal for the eight water molecules. The La-O distance was scanned with fixed TIP3P water geometry.

Ab initio calculations were performed using the GAUSSIAN-98 package.⁶⁰ The PES scan was performed at the MP2 perturbation level of theory. The La atom was described by the LanL2MB basis set and its associated pseudopotential.⁶¹ Hydrogen and oxygen atoms were described by the 6-31G* basis set.⁶² As usual, the size of the chosen basis set is a compromise between the accuracy of electronic calculation and the size of the clusters used to parametrize or check the La-O potential, namely, this level of theory allowed *ab initio* calculations on a $\text{La}(\text{H}_2\text{O})_{24}^{3+}$ cluster.

C. Molecular dynamics simulations

1. Simulation details

Simulations of the hydrated La^{3+} ion have been carried out in the microcanonical *NVE* ensemble with our own de-

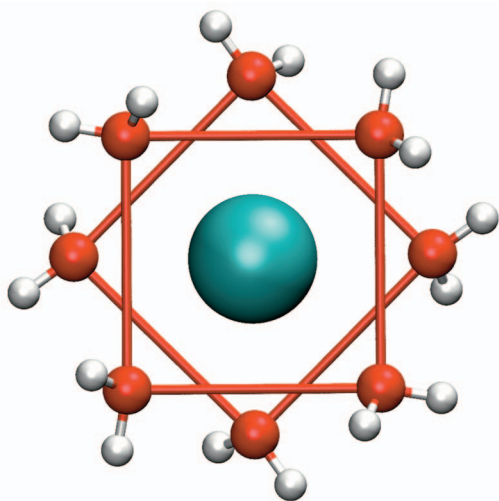


FIG. 1. (Color) Geometry of the La-(OH₂)₈³⁺ complex in the square antiprism (*D_{4d}*) geometry used to parametrize the interaction potentials from *ab initio* calculations.

veloped CLMD code.¹⁸ CLMD simulations were performed for 1 La³⁺ and 216 rigid water molecules in a cubic box at room temperature. A few tests with a larger simulation box (1000 water molecules) were performed. It gave virtually the same results, so that all the following reported results are for the former simulation box.

Periodic boundary conditions were applied to the simulation box. Long range interactions have been calculated by using the smooth particle mesh Ewald method.⁶³ The Coulombic energy divergence catastrophe is avoided by a *neutralizing plasma*^{64,65} implemented in Ewald summation by omitting the $\mathbf{k}=0$ term in the reciprocal space sum.⁶⁶ The net charge of the system induces a charged system term [$U_c = |\sum_i^N q_i|^2 / (8\epsilon_0 V \alpha^2)$].⁶⁷ In our case, this term results in adding a constant contribution to the total energy (since the net charge q and the volume V are constant in our simulations) corresponding to 0.2% of the total energy. However, the corresponding forces are not affected by this charged system term. Simulations were performed using a velocity-Verlet-based multiple time scale for the simulations with the TIP3P/P water model. Equations of motion were numerically integrated using a 1 fs time step. The system was equilibrated at 298 K for 2 ps. Production runs were subsequently collected for 3 ns. Computing time for each 3 ns trajectory varied from 21 h without explicit polarization to 30 h with explicit polarization on a 2.4 GHz AMD Opteron CPU. The average temperature was 299 K with a standard deviation of 10 K. To check if the system was correctly thermalized, we have performed simulations at different temperatures (within the liquid water domain). This gave linear van't Hoff plots for the La(H₂O)_{*i*-1}³⁺/La(H₂O)_{*i*}³⁺ water exchange reactions of the first hydration shell. This reflects negligible heat capacity influence and thus correct thermalization of the system. However, temperature influence is out of the scope of the present paper and will be published elsewhere.⁶⁸

2. Radial distribution function (RDF)

La-O and La-H RDFs were determined for the first and the second hydration shells; the CN is obtained by integrating the RDF,

$$\text{CN} = 4\pi\rho \int_{r_{\min}}^{r_{\max}} g(r)r^2 dr, \quad (17)$$

where r_{\min} and r_{\max} are the first and the second minima of the RDF, respectively, and ρ the atomic density of the system.

3. Mean residence time of water molecules

The procedure of Impey *et al.*⁶⁹ is generally used to determine the MRT of ligands when all ligands of a given shell have been exchanged. As the MRT of water molecules with Ln³⁺ ions is quite long (about 1 ns for La³⁺ at room temperature¹⁰), the “direct” method⁷⁰ was used to determine the MRTs of water molecules. The MRTs were thus estimated from an average of the time spent by a water molecule in the first hydration shell. As in the procedure of Impey *et al.*, a minimum time parameter ($t^*=2.0$ ps) defining a real “exchange” was introduced. For consistency, the same protocol was used to estimate the MRTs for the second hydration shell.

III. RESULTS AND DISCUSSION

A. Comparison of La-O interaction potentials

Three potentials were parametrized (see Sec. II A): Exp [Eq. (10)], Buck6 [Eq. (11)], and TF [Eq. (12)], while the Kit and Kit-TIP3P/P [Eq. (13)] potentials were used with published parameters (see Sec. II A). MD simulations were performed at room temperature with these potentials and explicit polarization. These results are here first compared with available published $r_{\text{La-O}}$ experimental values, and to be expected CN=9 (Table II). We will give more details on Buck6 MD simulations (i.e., MD simulations using the Buck6 potential) because it gives the best results (among our parametrized potentials), while the others (Exp, TF, Kit, and Kit-TIP3P/P) were used for comparison.

Quite surprisingly, the simplest (Exp) La-O pair IP gave relatively good results: $r_{\text{La-O}}^{(1)} = 2.59$ Å to be compared with 2.54 Å (Ref. 22) and 2.56 Å (Ref. 29) average La-O distance obtained by EXAFS spectroscopy (Table II). The CN = 8.77 calculated coordination number is of the correct order of magnitude. The Exp potential was parametrized only on *ab initio* calculations of La(H₂O)₈³⁺, since this potential form cannot reproduce the shape of the energy curves of the bigger La(H₂O)₈³⁺ clusters, where a slightly attractive contribution is present in the 2.5–5.0 Å La-O distance range. Unfortunately, exponential function cannot account for such negative contributions. Nevertheless, note that the good results of the MD simulations indicate that polarization is enough to account for most of the multibody attractive effects, since Exp was parametrized on the La³⁺-OH₂ two-body system.

For the previously mentioned reasons, we kept the exponential repulsive term and added an $(-1/r^6)$ attractive term: this is the Buck6 potential. We fitted all the parameters, now

TABLE II. Hydration properties of La^{3+} in aqueous solution at room temperature.

	$r_{\text{La-O}}^{(1)a}$	CN ^{(1)b}	MRT ^{(1)c}	$r_{\text{La-O}}^{(2)a}$	CN ^{(2)b}	MRT ^{(2)c}
Exp ^a	2.59	8.77	201	4.85	22.4	8.7
Buck6 ^d	2.52(2.50/2.58) ^c	9.02	1082	4.65	18.8	7.6
TF ^d	2.65	10.2	176	4.75	24.1	7.4
Kit ^d	2.55	8.76	207	4.83	21.4	5.7
Kit-TIP3P/P ^d	2.56	8.92	401	4.78	19.6	7.2
Exp _{up} ^f	2.46	9.02	610	4.60	18.1	7.5
Buck6 _{up} ^f	2.56	10.0	910	4.70	20.4	7.1
TF _{up} ^f	2.62	12.0	998	4.75	26.3	7.9
QM/MM MD ^g	...	9–10	>250	...	18–28	8.4
MD ^h	2.56	8.90	980	4.68	15.9	...
CPMD ⁱ	2.52	8.5
EXAFS ^j	2.54	9.20
EXAFS ^k	2.56(2.515/2.64) ^c	9(6+3)	...	4.63	18	...
EXAFS ^l	2.545	9
EXAFS ^m	2.56	12
XRD ⁿ	2.57	8	...	4.7	13	...
XRD ^o	2.58	9.13	...	5
XRD ^p	2.48	8	...	4.7

^aFirst ($r_{\text{La-O}}^{(1)}$) and second ($r_{\text{La-O}}^{(2)}$) maximum peak of La–O RDFs (in Å).

^bCoordination number of the first (CN⁽¹⁾) and second (CN⁽²⁾) hydration shells.

^cMRT of water molecule in the first (MRT⁽¹⁾) and second (MRT⁽²⁾) hydration shells (in ps).

^dPresent study with the TIP3P/P (polarizable) water model.

^eMean value of two different distances corresponding to a CN of 9=6+3.

^fPresent study with the TIP3P (unpolarizable) water model.

^gQM/MM MD (Ref. 14).

^hMD on the $\text{La}(\text{H}_2\text{O})_{60}^{3+}$ cluster (Ref. 10).

ⁱCPMD on LaCl_3 in aqueous solution (Ref. 15).

^jEXAFS ($L_{\text{II}}-L_{\text{III}}$ edge), 0.25 mol l⁻¹ Cl⁻ (Ref. 22).

^kEXAFS and LAXS (L_{II} edge), 3.856 mol l⁻¹ ClO₄⁻ (Ref. 29).

^lEXAFS (L_{III} edge), 0.8094 mol l⁻¹ $\text{La}(\text{ClO}_4)_3$ (Ref. 30).

^mEXAFS (L_{III} edge), 0.05–0.20 mol l⁻¹ LaCl_3 (Ref. 31).

ⁿXRD, 9.16 mol l⁻¹ ClO₄⁻ (Ref. 32).

^oXRD, 3.808 mol kg⁻¹ LaCl_3 (Ref. 33).

^pXRD, 1.54–2.67 mol kg⁻¹ LaCl_3 (Ref. 34).

also using $\text{La}(\text{H}_2\text{O})_8^{3+}$ clusters. For this reason, these parameters also account for short range multibody effects. We then further slightly refined the parameters by using trial MD simulations. The obtained Buck6 La–O distance (2.52 Å) is in reasonable agreement with published EXAFS results [2.54 Å (Ref. 22) and 2.56 Å (Ref. 29)] and with a recent MD value obtained for $\text{La}(\text{H}_2\text{O})_{60}^{3+}$ clusters [2.56 Å (Ref. 10)]. The CN (9.02) of the first hydration shell is also in good agreement with experimental evidence and with the CN (8.9) obtained by Clavaguéra *et al.*¹⁰ in their MD study of $\text{La}(\text{H}_2\text{O})_{60}^{3+}$. Note that they have used a 14-7 repulsive-dispersion term, while we used an exponential-6 one.

The minimum energy of the $\text{La}^{3+}-\text{OH}_2$ two-body system is at about 2.3 Å, while the Buck6 potential is slightly attractive for distances greater than 2.6 Å. However, at these distances the Buck6 potential energy is less than 10% of the total energy and less than 6% at distances more than 4 Å that correspond to the beginning of the second hydration shell (Fig. 2). This confirms that most of the multibody effects are in the explicit polarization term and not in fitted parameters. Namely, La-water polarization energy is 42%, 43%, and 23% of the total energy at 2.3, 2.6, and 4 Å, respectively, while

for water-water interaction it is about 5%–10% of the total interaction.⁷¹ The Buck6 potential is an important contribution term to the total energy only at very short distances. It accounts for repulsion. Since the $1/r^6$ term is here attractive, most of this attraction is more of physical origin, i.e., dipole-dipole interactions rather than an empirical term for compensating the exponential one. This results in an overall attractive Buck6 potential at the distances indicated just above. This is in contrast with the always positive Kit IPs [Eq. (13)]. Nevertheless, for both (Buck6 and Kit) potentials the exponential term is shifted (by about 0.14 and 0.07 Å, respectively) to larger distances, as compared to the overall repulsive wall. This might very well reflect that the $(1/r^n)$ attractive terms also partially correct the shape of the repulsive term because its (exponential) form is not completely appropriate.

By comparing now the MRTs of water molecules in the first hydration shell, the Buck6 potential appears to give a MRT five times greater than that obtained with the Exponential. Actually, the first peak of the La–O RDF obtained with the Buck6 potential is narrower and more symmetric than that obtained with the Exponential (Fig. 2). This re-

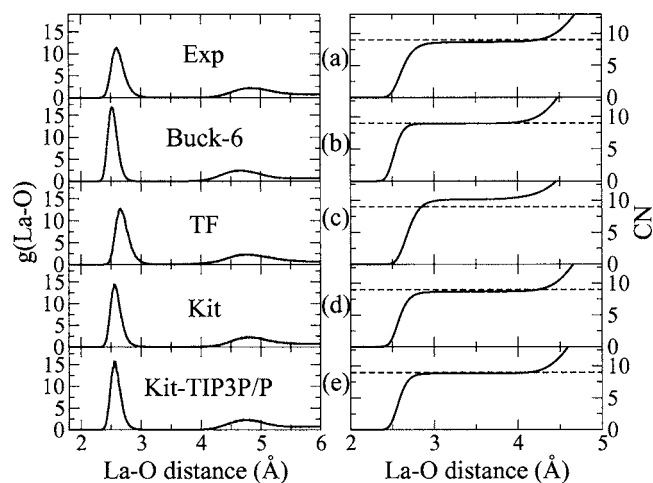


FIG. 2. La-O radial distribution functions (left panels) and coordination numbers (right panels) obtained for the different interaction potentials: (a) Exp, (b) Buck6, (c) TF, (d) Kit, and (e) Kit-TIP3P/P potentials.

flects that water molecules are more strongly bounded to La^{3+} and less likely to exchange when using the Buck6 potential.

The TF potential provided quite poor results. It overestimates the La-O distance of the first hydration shell by about 0.1 Å. It also overestimates the CN (see Table II). Attempts to slightly refine these parameters (as done for the Buck6 potential) did not improve the MD simulation results much. It seems surprising that adding terms to Buck6 for obtaining TF and refitting all of them did not improve the model. Actually, this is originated in the fitting, which results now in a $C_{6,ij}^{\text{TF}}/r^6$ repulsive term ($C_{6,ij}^{\text{TF}} < 0$). We did not attempt to add further constraints in the fitting procedure, as typically $C_{6,ij}^{\text{TF}} > 0$, because the Kit potential already has an attractive $1/r^6$ term (see below) and then we can only recover this potential. Furthermore, the TF potential has the most important attractive contribution among the tested potentials. This is rather a consequence of the incorrect mathematical form of the main repulsion term, which explains the poor results obtained with the TF potentials. Note that repulsive $C_{6,ij}$ terms are quite common and can provide good TF potentials for doubly charged transition metals.⁷²

In conclusion, among our three potentials, i.e., the Exp, the Buck6, and the TF potentials, MD simulations using the Buck6 potential with explicit polarization better reproduce available well established experimental information.

The Buck6 potential is now compared with the published Kit¹⁷ and the Kit-TIP3P/P potentials (Table II). The analytical expression of the Kit potential is similar to that of the TF potential, since the dispersion-exchange term is negligible, as compared to the repulsion and dispersion terms. However, the La-O distances and the CNs obtained for the first hydration shell by using the Kit and the Kit-TIP3P/P potentials are different from those obtained by using the TF potential. The La-O distance obtained with the Kit potential (2.55 Å) is in very good agreement with experimental values for the first hydration shell (Table II), whereas a La-O distance of 2.65 Å was calculated with the TF potential. Note that we did not optimize the Kit potential parameters: we took pub-

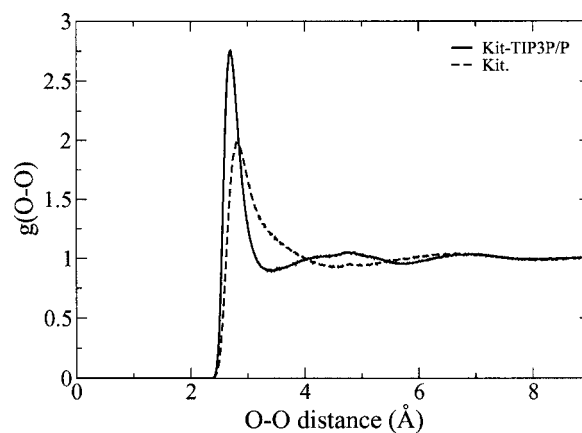


FIG. 3. O-O radial distribution functions obtained for $\text{La}(\text{H}_2\text{O})_{216}^{3+}$ MD simulations with the Kit-TIP3P/P (solid line) and the Kit (dash line) potentials.

lished values for C_6 , C_8 , C_{10} , C , C^{de} , γ , and γ^{de} (see Sec. II A), which, in principle, reflect atomic properties. This means that they were not specially fitted on $\text{La}^{3+}/\text{H}_2\text{O}$ *ab initio* results. The Kit potential is thus only defined by a repulsion-dispersion term depending essentially on the van der Waals radii of interacting species. The Kit La-O IP curve appears to be between the Exp and Buck6 ones for $\text{La}(\text{H}_2\text{O})^{3+}$ (data not shown). Note that the Exp, Buck6, and Kit potentials give similar MD results for the structural properties of the first hydration shell (Table II). Furthermore, the Kit MRT is of the same order of magnitude as the Exp MRT, i.e., 200 ps. It is about five times smaller than the Buck6 MRT.

The difference might originate from the La-O IP or from the water model. To check this, the TIP3P/P water model was used, namely, MD simulations were performed by using the Kit-TIP3P/P potential. Indeed, instead of describing the O-O IP with the Kit potential, the O-O interaction was described with the TIP3P/P. This changed the MD simulation results (Table II). Namely, the Kit O-O RDF is composed of two peaks centered at 2.82 and at about 6.60 Å, while the Kit-TIP3P/P model gives three O-O RDF peaks at 2.70, 4.80, and about 6.80 Å (Fig. 3). These last results are in good agreement with neutron diffraction results obtained for liquid water at 298 K.⁷³ The repulsion term of the Kit potential for the water-water interaction is more important than that of the 12-6 LJ potential describing the water-water interaction in liquid water. The difference in the repulsion between the two models is also reflected in the MRT values for the first hydration shell, i.e., the Kit MRT is twice smaller than the Kit-TIP3P/P MRT. It appears that the Kit-TIP3P/P and the Buck6 MD simulations provide the closest results, as compared to those using the other tested potentials. Thus, the Buck6 and the Kit-TIP3P/P potentials provide better agreement with experimental data among the five potentials tested to simulate the La^{3+} hydration in aqueous solution with explicit polarization.

The Buck6 and Kit-TIP3P/P potentials nevertheless give slightly different results for the second hydration shell: the Buck6 MD simulations provide a slightly smaller second hydration shell La-O distance and CN. Compared with experi-

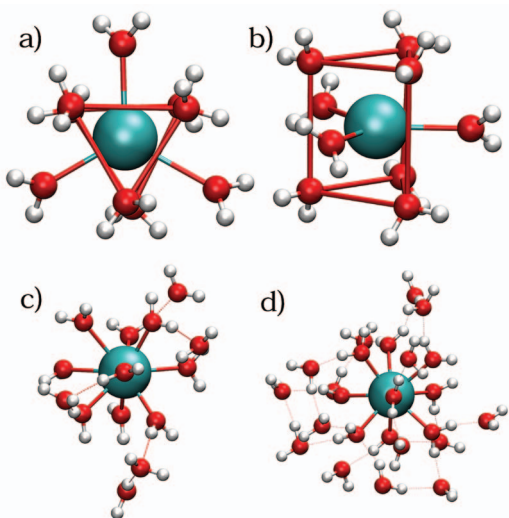


FIG. 4. (Color) Some snapshots of reduced hydrated La^{3+} ion clusters extracted from MD simulations done in bulk water: [(a) and (b)] $\text{La}(\text{H}_2\text{O})_9^{3+}$, (c) $\text{La}(\text{H}_2\text{O})_{14}^{3+}$, and (d) $\text{La}(\text{H}_2\text{O})_{24}^{3+}$.

mental data $r_{\text{La-O}}^{(2)}$, the Buck6 value (4.65 Å) is closer to recent EXAFS (4.63 Å) (Ref. 29) and older XRD (4.70 Å) (Ref. 32) data than the Kit-TIP3P/P one (4.78 Å). These small differences are also reflected in $\text{MRT}^{(1)}$, the water residence time in the first La^{3+} hydration shell. $\text{MRT}^{(1)}$ is correlated to the water exchange mechanism, which involves the second hydration shell. It is important to notice that the Buck6 potential has a simple analytical form that will allow us to easily extrapolate our results to other lanthanides. To illustrate that, we used published ionic radii⁷⁴ in an attempt to extrapolate the La–O Buck6 parameters to the other lanthanides; i.e., we changed parameters to visually shift the La–O IP by the difference between the ionic radii. The corresponding MD simulations reproduced published $r_{\text{Ln-O}}$ distances and the decrease in CN with atomic number in the Ln series (from CN=9 to 8).⁷⁵

Finally, we chose the Buck6 potential as our favorite potential since it provides correct structural and dynamical informations and can be extended to other atoms in the lanthanide series. Its validity was further evaluated by comparing the *ab initio* (MP2) and model calculated energies of small clusters, i.e., $(\text{La}-\text{OH}_2)_n^{3+}$ with $n=1,2,3,8$, and bigger clusters extracted from MD simulations, $(\text{La}-\text{OH}_2)_n^{3+}-(\text{H}_2\text{O})_m$ with $n=8$ or 9 and $n+m=9,14,24$ (Fig. 4). A good agreement between the MP2 and model energies is obtained for all the studied clusters with negative energies (Fig. 5). Some points are not on the $E_{\text{model}}=E_{\text{ab initio}}$ line: they correspond to positive energies calculated in the repulsion walls. We indeed endeavor to reproduce the energies corresponding to La–O distances more than 2 Å, since the closest observed La–O distance was 2.20 Å in our MD simulations at 299 K. Moreover, this comparison shows that the correlation between MP2 and model energies is better when increasing the number of water molecules, e.g., the relative difference between model and *ab initio* energies is 0.6% for the $\text{La}(\text{H}_2\text{O})_{24}^{3+}$ cluster. This also confirms the good transferability of the TIP3P/P water model together with the reliability of the implemented polarization.

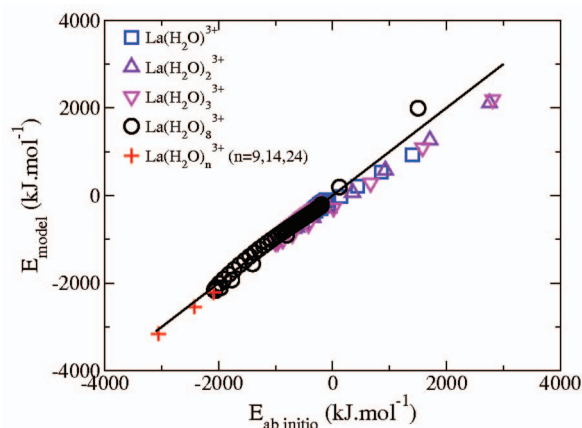


FIG. 5. (Color) *Ab initio* (MP2) vs polarizable Buck6 model total internal energies for various $\text{La}(\text{H}_2\text{O})_n^{3+}$ clusters ($n=1-24$).

In conclusion, increasing the number of water molecules improves the correlation between MP2 and model energies. The Buck6 potential is thus appropriate to correctly describe the La–O interaction for simulations of La^{3+} in aqueous solution.

B. Polarization effects

As for the TIP3P/P water model, we compared several potential forms to describe the La–O interaction without explicit polarization and with the TIP3P water model (see Sec. II A), i.e., the Exp_{up} , the Buck6_{up} , and the TF_{up} potentials, where the subscript “up” is for unpolarizable. For the Exp_{up} potential, a La–O distance of 2.46 Å and a CN of 9 were found for the first hydration shell (Table II). The second hydration shell is centered at 4.60 Å with 18 water molecules: only the first shell is really incorrect, it is too small by at least 0.06 Å. For the Buck6_{up} potential, we have obtained a La–O distance of 2.56 Å and a CN of 10 (instead of the expected value of 9) for the first hydration shell and a La–O distance of 4.70 Å with 20 water molecules for the second hydration shell. For the TF_{up} potential, a La–O distance of 2.62 Å and a CN of 12 for the first hydration shell are obtained, and a La–O distance of 4.75 Å and a CN of 26 for the second hydration shell are also obtained. The results obtained with the TIP3P water model (Table II) are not consistent with those obtained with the TIP3P/P model, neither with experimental data. The Buck6_{up} potential is the only potential that gives results in good agreement with experimental La–O distance.^{22,29} However, with this potential, the CN is too large, i.e., a CN of 10 instead of 9. On the other hand, the Exp_{up} potential gives a consistent CN for the first hydration shell, as compared to the experimental and computed CN, but the calculated La–O distance is too small, i.e., the La–O distance is underestimated by about 0.1 Å. The TF_{up} does not give correct results at all (Table II). In conclusion, without explicit polarization we did not succeed to reproduce both correct distance and CN for the first hydration shell.

This strengthens the view that polarization holds an important role in the hydration of La^{3+} , and this is poorly ac-

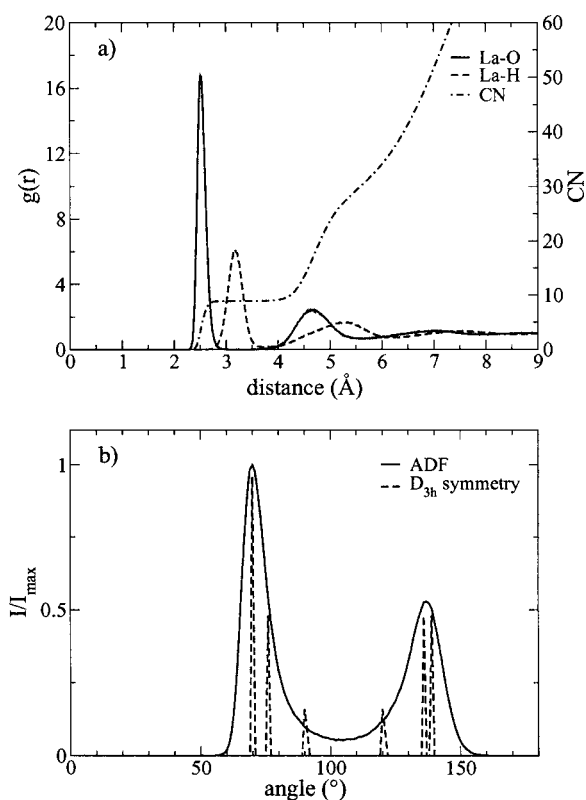


FIG. 6. Top: Radial distribution functions of La–O (solid line), La–H (dash line), and CN (dash-dot line). Bottom: Angular distribution function of O–La–O in the first hydration shell compared to ADF of the D_{3h} TTP geometry.

counted for by fitting pair IPs. Taking into account polarization explicitly is thus essential to describe correctly the hydration of La^{3+} in aqueous solution.

C. Structural properties

Here we describe in some detail the structural properties obtained with the Buck6-TIP3P/P model. La–O RDF shows two well-defined peaks corresponding to the first and the second hydration shells [Fig. 6(a)]. The first and second peaks are centered at 2.52 and at 4.65 Å, respectively (Table II), while the third hydration shell is not well defined. As the other hydration shells are not defined, we can conclude that La^{3+} has an effect only on the first three hydration shells (to about 8 Å). At 299 K, the calculated La–O distance of the first hydration shell is in good agreement with experimental and computed values shown in Table II. The mean associated coordination number of 9.02 is an average of different distribution complexes with CN=9 and 10. CN=9 is the most frequent, i.e., 98.1% and 1.9% for $\text{La}(\text{H}_2\text{O})_9^{3+}$ and $\text{La}(\text{H}_2\text{O})_{10}^{3+}$, respectively. Also the La–O distance and coordination number of the second hydration shell, i.e., 18.8 water molecules at 4.65 Å, are consistent with the experimental and computed values (Table II) as already outlined above. Angular distribution function (ADF) of O–La–O shows two peaks [Fig. 6(b)]. The first peak is located at 70° and the second at 137°. ADF obtained from MD simulations is consistent with ADF obtained from $\text{La}(\text{H}_2\text{O})_9^{3+}$ complex in the D_{3h} tricapped trigonal prism (TTP) geometry [Figs. 4(a) and

4(b)]. Fitting the La–O distances of the first hydration shell with two Gaussian distribution functions, two La–O distances of 2.50 and 2.58 Å (with corresponding CNs of 6 and 3) have been calculated corresponding to two different water molecule populations: the capping (3) and the prismatic (6) water molecules. ADF is also in good agreement with ADF for a TTP geometry obtained by Chaussedent *et al.*⁷⁶ for their MD study of Eu^{3+} in aqueous solution.

The La–H peak of the first hydration shell is centered at 3.17 Å. The number of H in the first hydration shell is 18.5 corresponding to about twice the number of water molecules in the first shell. It is less straightforward to determine the limit of the second hydration shell from La–H RDF, since the two corresponding peaks are not entirely separated.

The La–O and CN results we obtained by using the Buck6 potential for the second hydration shell (Table II) are consistent with experimental data obtained by large angle x-ray scattering (LAXS) spectroscopy,²⁹ i.e., a La–O distance of 4.63 Å and a CN of 18.

D. Dynamical properties

Water exchanges between the first and the second hydration shells obtained with Buck6-TIP3P/P MD simulations are observed and detailed as follows (16 water exchanges). The main reaction is the synchronous leaving and incoming of a water molecule (Fig. 7). A transient complex $\text{La}(\text{H}_2\text{O})_{10}^{3+}$ is observed during the exchange with a lifetime of up to 10 ps. The starting species is $\text{La}(\text{H}_2\text{O})_9^{3+}$ of approximately TTP D_{3h} structure composed of three parallel triangles. The top and bottom ones are symmetric, while the medium one is a little bigger and is opposite (rotation of 60°) to the two other ones. For this reason, this structure can be named “6+3.” Note that looking to a rectangle face of TTP, it can also be seen as a deformed D_{4d} square antiprism (SAP), the classical “2×4” geometry of $\text{Ln}(\text{H}_2\text{O})_8^{3+4}$ with the ninth water molecule outside the center of one face, a “2×4+1” or a “4+(4+1)” geometry. In the medium triangle, the La–O distances are slightly bigger (Table II) corresponding to weaker bonds. Indeed, the exchanges are observed in this medium plane. The $\text{O}_{\text{in}}\text{--La--O}_{\text{leav}}$ angle is about 180°, when the incoming water molecule ($\text{H}_2\text{O}_{\text{in}}$) is arriving and the leaving one ($\text{H}_2\text{O}_{\text{leav}}$) is still here. Resulting $\text{Ln}(\text{H}_2\text{O})_{10}^{3+}$ have a deformed D_{4d} SAP structure, i.e., the classical geometry of $\text{Ln}(\text{H}_2\text{O})_8^{3+}$ with now two supplementary water molecules outside the center of each square, a “2×(4+1)” geometry. These two extra molecules are actually the incoming and leaving water molecules. When the leaving water molecule has gone away, $\text{Ln}(\text{H}_2\text{O})_9^{3+}$ comes back to the TTP geometry.

Helm and Merbach³⁵ suggested a dissociative interchange for water exchanges on $\text{Nd}(\text{H}_2\text{O})_9^{3+}$, i.e., a concerted exchange with a weak dissociative character, via a $\text{Nd}(\text{H}_2\text{O})_8^{3+}$ transient complex. However, the water exchange reaction pathway for lanthanide ions is not clearly defined.^{7,19,35,40} Moreover, the reaction pathway we have observed could not be compared to the one suggested by Helm and Merbach since the two main configurations we have ob-

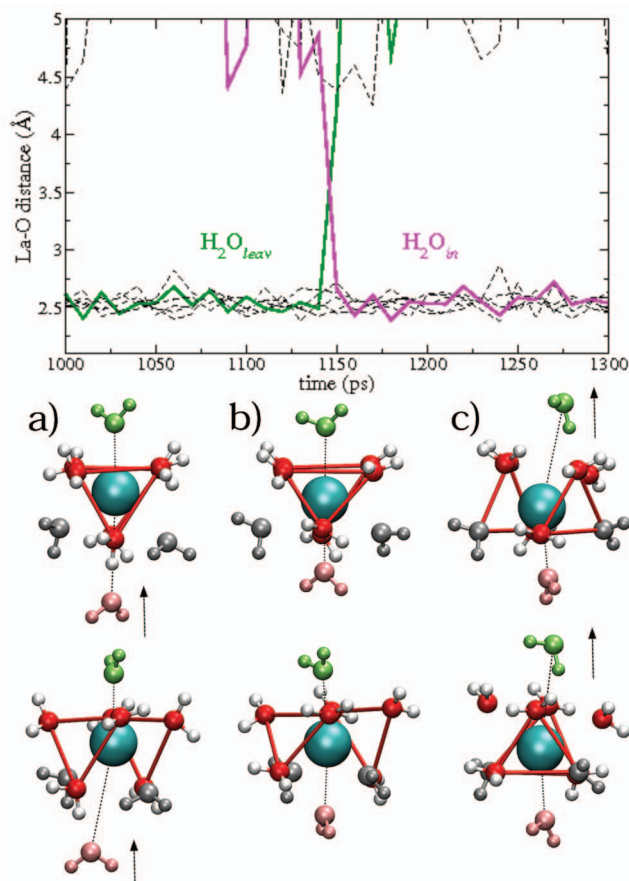


FIG. 7. (Color) La–O distance of selected water molecules as a function of the simulation time showing a synchronous water exchange between the *green* and the *pink* water molecules. (a) Before the water exchange, the *green* and the two *gray* water molecules are in the medium triangle. (b) During the water exchange, the *green* and the *pink* water molecules are at the same distance of La^{3+} . (c) After the water exchange, the two *gray* water molecules are now included in the prism, and the *pink* water molecule is in the medium triangle (for clarity, two orientation views are shown).

served are $\text{La}(\text{H}_2\text{O})_9^{3+}$ and $\text{La}(\text{H}_2\text{O})_{10}^{3+}$. The reaction pathway proposed by Helm and Merbach is for the $\text{Nd}(\text{H}_2\text{O})_9^{3+}/\text{Nd}(\text{H}_2\text{O})_8^{3+}$ exchange.

The calculated MRT of water molecules at 299 K is about 1 ns (Table II). Unfortunately, there are no experimental data of water molecule MRT in the aqueous solution of La^{3+} to compare with as already outlined in the Introduction. Water exchange rate constants have been extracted from ^{17}O NMR measurements of Ln^{3+} aqueous solutions.^{3,19,35–40} These rate constants appeared to decrease with the atomic number. Unfortunately, it could only be measured for heavy lanthanides, whose structure is $\text{Ln}(\text{H}_2\text{O})_8^{3+}$. The kinetic effect is indeed not sufficient to enable the determination of water exchange rate constants for light lanthanides ($\text{Ln}=\text{La}$ to Sm).^{5,35} For this reason, extrapolation down to light $\text{Ln}(\text{H}_2\text{O})_9^{3+}$ species is highly hypothetical. Nevertheless, few authors proposed such extrapolation assuming a maximum value of the exchange rate constant and consequently a minimum value of MRT, for Gd^{3+} .³⁵ The ^{17}O NMR MRTs published for nine-coordinated Ln^{3+} are 2 ns [$\text{Pr}(\text{H}_2\text{O})_9^{3+}$], 2.5 ns [$\text{Nd}(\text{H}_2\text{O})_9^{3+}$],³⁵ 943 ps (Ref. 47) and 833 ps (Ref. 40) [$\text{Gd}(\text{H}_2\text{O})_9^{3+}$], and 2.02 ns [$\text{Tb}(\text{H}_2\text{O})_9^{3+}$].^{37,77,78} These values

indicate that MRTs are 1 ns to a few nanoseconds. A MRT of 980 ps has been obtained for a 1 ns MD simulation on a $\text{La}(\text{H}_2\text{O})_{60}^{3+}$ cluster,¹⁰ a value very similar to the one we obtained. Nevertheless, experimental confirmations are still needed.

IV. CONCLUSIONS AND OUTLOOKS

This work, as can be argued by a careful literature examination, clearly shows that explicit polarization is needed for studying La^{3+} in liquid water by means of CLMD simulations and that the parametrized La–O interactions should reproduce high level *ab initio* calculations, preferably on clusters with realistic manybody effects. However, to our best knowledge, these methodologies have not been used in a single study based on MD simulations with periodic boundary conditions to correctly simulate a liquid system. Taking into account all these aspects, we were able to correctly reproduce available experimental data, which strengthens the confidence in our approach and more precisely in pair IP energy forms and related parameters when combined with explicit polarization. Note that we used a simple model for water (TIP3P/P) and fixed atomic partial charges. Furthermore, we obtained from simulations supplementary insights on La^{3+} hydration for which there is still not undebated experimental information.

In the present work, several La–O IPs were parametrized in order to simulate the hydration of La^{3+} in aqueous solution: the Exp, Buck6, and TF potentials. The Buck6 potential is slightly negative in the 2.6–4.2 Å range for the two-body $\text{La}(\text{H}_2\text{O})_3^{3+}$ system. We should notice that potentials lacking this attractive contribution (Exp or Kit-TIP3P/P) are also able to provide reasonable results for the first hydration shell structure. The main difference is in the second hydration shell and associated properties, in particular, MRTs. The attractive contribution of Buck6 is associated with longer water residence times in the La^{3+} first hydration layer. That seems more in agreement with experimental information.

Most of the many-body effects were taken into account by explicit polarization, which was confirmed to be needed for reproducing both well established distances and CNs. Explicit polarization essentially decreases—and improves—the MD modeled La^{3+} first hydration shell coordination number and slightly decreases the size of the second hydration shell. It also increases the water molecule MRT in the first La^{3+} hydration shell. Note that other MD residence times obtained with other potentials described in this work are smaller and indeed probably too small. This reflects differences in the second hydration shell among MD results. We observed that the residence time essentially originates in the transient formation of $2 \times (4+1) \text{La}(\text{H}_2\text{O})_{10}^{3+}$ from $6+3 \text{La}(\text{H}_2\text{O})_9^{3+}$ in the course of a concerted water exchange.

It appears that a simple potential form describes correctly the $\text{La}^{3+}-\text{OH}_2$ interaction: the Buck6 potential only composed of a repulsion and a dispersion term. This simplicity will facilitate, in the future, extrapolation of parameters we have determined for the La–O interaction to the other Ln–O interactions ($\text{Ln}=\text{Ce}$ to Lu), since the Ln^{3+} hydration

properties in aqueous solution depend essentially on the Ln³⁺ ionic radius, and our Buck6 potential indeed essentially reflects ionic radius.

The present study encourages us to proceed further with other lanthanide ion hydration studies and with La³⁺ solvation in aqueous solutions containing anions and other cations.

ACKNOWLEDGMENT

The authors are grateful to Dr. Marie-Pierre Gageot for helpful discussions and suggestions. She initiated the project that produced the computer program used in the present work.

- ¹ W. Meier, P. Bopp, M. M. Probst, E. Spohr, and J. L. Lin, *J. Phys. Chem.* **94**, 4672 (1990).
- ² S. Galera, J. M. Lluch, A. Oliva, J. Bertran, F. Foglia, L. Helm, and A. E. Merbach, *New J. Chem.* **17**, 773 (1993).
- ³ L. Helm, F. Foglia, T. Kowall, and A. E. Merbach, *J. Phys.: Condens. Matter* **6**, A132 (1994).
- ⁴ T. Kowall, F. Foglia, L. Helm, and A. E. Merbach, *J. Phys. Chem.* **99**, 13078 (1995).
- ⁵ T. Kowall, F. Foglia, L. Helm, and A. E. Merbach, *J. Am. Chem. Soc.* **117**, 3790 (1995).
- ⁶ S. Chaussement and A. Monteil, *J. Chem. Phys.* **105**, 6532 (1996).
- ⁷ T. Kowall, F. Foglia, L. Helm, and A. E. Merbach, *Chem.-Eur. J.* **2**, 285 (1996).
- ⁸ F. M. Floris and A. Tani, *J. Chem. Phys.* **115**, 4750 (2001).
- ⁹ A. Chaumont and G. Wipff, *Inorg. Chem.* **43**, 5891 (2004).
- ¹⁰ C. Clavaguéra, R. Pollet, J. M. Soudan, V. Brenner, and J. P. Dognon, *J. Phys. Chem. B* **109**, 7614 (2005).
- ¹¹ S. R. Hughes, T.-N. Nguyen, J. A. Capobianco, and G. H. Peslherbe, *Int. J. Mass. Spectrom.* **241**, 283 (2005).
- ¹² C. Clavaguera, F. Calvo, and J.-P. Dognon, *J. Chem. Phys.* **124**, 074505 (2006).
- ¹³ A. Ruas, P. Guilbaud, C. Den Auwer, C. Moulin, J.-P. Simonin, P. Turq, and P. Moisy, *J. Phys. Chem. A* **110**, 11770 (2006).
- ¹⁴ B. M. Rode and T. S. Hofer, *Pure Appl. Chem.* **78**, 525 (2006).
- ¹⁵ T. Ikeda, M. Hirata, and T. Kimura, *J. Chem. Phys.* **122**, 244507 (2005).
- ¹⁶ H.-S. Kim, *Chem. Phys. Lett.* **330**, 570 (2000).
- ¹⁷ A.-L. Derepas, J.-M. Soudan, V. Brenner, and P. Millié, *J. Comput. Chem.* **23**, 1013 (2002).
- ¹⁸ M. Souaille, D. Borgis, and M.-P. Gageot, MDVRY, molecular dynamics program developed at the University of Evry, 2006 (for more information please contact Marie-Pierre Gageot at gageot@ccr.jussieu.fr).
- ¹⁹ L. Helm and A. E. Merbach, *Coord. Chem. Rev.* **187**, 151 (1999).
- ²⁰ J.-P. Blaudeau, S. A. Zygmunt, L. A. Curtiss, D. T. Reed, and B. E. Bursten, *Chem. Phys. Lett.* **310**, 347 (1999).
- ²¹ T. Yang, S. Tsushima, and A. Susuki, *J. Phys. Chem. A* **105**, 10439 (2001).
- ²² P. Allen, J. J. Bucher, D. K. Shuh, N. M. Edelstein, and I. Craig, *Inorg. Chem.* **39**, 595 (2000).
- ²³ P. Lindqvist-Reis, R. Klenze, G. Schubert, and T. Fanghänel, *J. Phys. Chem. B* **109**, 3077 (2005).
- ²⁴ P. Lindqvist-Reis, C. Walthers, R. Klenze, A. Eichhofer, and T. Fanghanel, *J. Phys. Chem. B* **110**, 5279 (2006).
- ²⁵ P. Vitorge, V. Phrommavanh, B. Siboulet, D. You, T. Vercouter, M. Descostes, C. J. Marsden, C. Beaucaire, and J.-P. Gaudet, *C. R. Chim.* (to be published).
- ²⁶ R. Silva, G. Bidoglio, M. Rand, P. Robouch, H. Wanner, and I. Puigdomenech, *Chemical Thermodynamics of Americium* (OECD NEA Data Bank, Issy-les-Moulineaux, 1995).
- ²⁷ P. Vitorge and H. Capdevila, *Radiochim. Acta* **91**, 623 (2003).
- ²⁸ P. Vitorge, *Chimie des Actinides (Chemistry of Actinides)* (Techniques de l'ingénieur, Paris, 1999), Vol. BN2.
- ²⁹ J. Näslund, P. Lindqvist-Reis, I. Persson, and M. Sandström, *Inorg. Chem.* **39**, 4006 (2000).
- ³⁰ S.-I. Ishiguro, Y. Umebayashi, K. Kato, R. Takahashi, and K. Ozutsumi, *J. Chem. Soc., Faraday Trans.* **94**, 3607 (1998).
- ³¹ J. A. Solera, J. Garcia, and M. G. Proietti, *Phys. Rev. B* **51**, 2678 (1995).
- ³² G. Johansson and H. Wakita, *Inorg. Chem.* **24**, 3047 (1985).
- ³³ A. Habenschuss and F. H. Spedding, *J. Chem. Phys.* **70**, 3758 (1979).
- ³⁴ L. S. Smith and D. L. Wertz, *J. Am. Chem. Soc.* **97**, 2365 (1975).
- ³⁵ L. Helm and A. E. Merbach, *Chem. Rev. (Washington, D.C.)* **105**, 1923 (2005).
- ³⁶ C. Cossy and A. E. Merbach, *Pure Appl. Chem.* **60**, 1785 (1988).
- ³⁷ C. Cossy, L. Helm, and A. E. Merbach, *Inorg. Chem.* **27**, 1973 (1988).
- ³⁸ P. Caravan and A. E. Merbach, *Chem. Commun. (Cambridge)* **1997**, 2147.
- ³⁹ H. Ohtaki, *Monatsch. Chem.* **132**, 1237 (2001).
- ⁴⁰ L. Helm and A. E. Merbach, *J. Chem. Soc. Dalton Trans.* **2002**, 633.
- ⁴¹ C. Cossy, L. Helm, and A. E. Merbach, *Inorg. Chim. Acta* **139**, 147 (1987).
- ⁴² C. Cossy, L. Helm, and A. E. Merbach, *Inorg. Chem.* **28**, 2699 (1989).
- ⁴³ D. P. Fay, D. Litchinsky, and N. Purdie, *J. Phys. Chem.* **73**, 544 (1969).
- ⁴⁴ R. V. Southwood-Jones, W. L. Earl, K. E. Newman, and A. E. Merbach, *J. Chem. Phys.* **73**, 5909 (1980).
- ⁴⁵ B. T. Thole, *Chem. Phys.* **59**, 341 (1981).
- ⁴⁶ P. van Duijnen and M. Swart, *J. Phys. Chem. A* **102**, 2399 (1998).
- ⁴⁷ *Handbook of Chemistry and Physics* (CRC, Boca Raton, FL, 1996).
- ⁴⁸ R. Car and M. Parrinello, *Phys. Rev. Lett.* **55**, 2471 (1985).
- ⁴⁹ M. Sprik, *J. Phys. Chem.* **95**, 2283 (1991).
- ⁵⁰ J. E. Lennard-Jones, *Proc. R. Soc. London, Ser. A* **106**, 463 (1924).
- ⁵¹ W. L. Jorgensen, J. Chandrasekhar, J. D. Madura, R. W. Impey, and M. L. Klein, *J. Chem. Phys.* **79**, 926 (1983).
- ⁵² J. Caldwell, L. X. Dang, and P. A. Kollman, *J. Am. Chem. Soc.* **112**, 9144 (1990).
- ⁵³ J. W. Caldwell and P. A. Kollman, *J. Phys. Chem.* **99**, 6208 (1995).
- ⁵⁴ R. Armunanto, C. F. Schwenk, A. H. B. Setiaji, and B. M. Rode, *Chem. Phys.* **295**, 63 (2003).
- ⁵⁵ R. A. Buckingham, *Proc. R. Soc. London, Ser. A* **168**, 264 (1938).
- ⁵⁶ F. G. Fumi and M. P. Tosi, *J. Phys. Chem. Solids* **25**, 31 (1964).
- ⁵⁷ M. P. Tosi and F. G. Fumi, *J. Phys. Chem. Solids* **25**, 45 (1964).
- ⁵⁸ A. I. Kitaygorodsky, *Tetrahedron* **14**, 230 (1961).
- ⁵⁹ A.-L. Derepas, Ph.D. thesis, Université Paris XI, 2001.
- ⁶⁰ M. Frisch, G. Trucks, H. Schlegel *et al.*, GAUSSIAN 98, Revision A.9, Gaussian, Inc., Pittsburgh, PA, 1998.
- ⁶¹ P. J. Hay and W. R. Wadt, *J. Chem. Phys.* **82**, 299 (1985).
- ⁶² P. C. Hariharan and J. A. Pople, *Theor. Chim. Acta* **28**, 213 (1973).
- ⁶³ U. Essmann, L. Perera, M. L. Berkowitz, T. Darden, H. Lee, and L. G. Pedersen, *J. Chem. Phys.* **103**, 8577 (1995).
- ⁶⁴ G. Hummer, L. Pratt, and A. Garcia, *J. Phys. Chem.* **100**, 1206 (1996).
- ⁶⁵ S. Bogusz, T. E. C. III, and B. R. Brooks, *J. Chem. Phys.* **108**, 7070 (1998).
- ⁶⁶ D. Frenkel and B. Smit, *Understanding Molecular Simulation* (Academic, New York, 1996).
- ⁶⁷ T. Matthey, Plain Ewald and PME (2005), available at <http://protomol.sourceforge.net/ewald.pdf>
- ⁶⁸ M. Duvail, R. Spezia, T. Cartailleur, and P. Vitorge *Chem. Phys. Lett.* (submitted).
- ⁶⁹ R. W. Impey, P. A. Madden, and I. R. McDonald, *J. Phys. Chem.* **87**, 5071 (1983).
- ⁷⁰ T. S. Hofer, H. T. Tran, C. F. Schwenk, and B. M. Rode, *J. Comput. Chem.* **25**, 211 (2004).
- ⁷¹ A. Amadei, M. Aschi, R. Spezia, and A. Di Nola, *J. Mol. Liq.* **101**, 181 (2002).
- ⁷² G. Chillemi, P. D'Angelo, N. Pavel, N. Sanna, and V. Barone, *J. Am. Chem. Soc.* **124**, 1968 (2002).
- ⁷³ A. K. Soper, *Chem. Phys.* **258**, 121 (2000).
- ⁷⁴ R. D. Shannon, *Acta Crystallogr., Sect. A: Cryst. Phys., Diffr., Theor. Gen. Crystallogr.* **32**, 751 (1976).
- ⁷⁵ M. Duvail, Ph. D. thesis, Université Paris XI, (2007).
- ⁷⁶ S. Chaussement, A. Monteil, M. Ferrari, and L. D. Longo, *Philos. Mag. B* **77**, 681 (1998).
- ⁷⁷ H. Ohtaki and T. Radnai, *Chem. Rev. (Washington, D.C.)* **93**, 1157 (1993).
- ⁷⁸ G. Laurenczy and A. E. Merbach, *Helv. Chim. Acta* **71**, 1971 (1988).